ISSN 1087-6596, Glass Physics and Chemistry, 2024, Vol. 50, No. 1, pp. 36–46. © Pleiades Publishing, Ltd., 2024.
Russian Text © The Author(s), 2024, published in Fizika i Khimiya Stekla.

Concentration Effect of Glass Former on the Lumenescene Properties of Tb^{3+}-Ions Doped $Na_2O–CaO–B_2O_3–TeO_2$ Glasses for Laser Applications

M. Shoaib[a], Ata Ullah[b], Abdullah A. A. Mohammed[c], S. M. Wabaidur[c], F. Qiao[a], I. Khan[b, *], G. Rooh[b], and I. Ullah[b]

[a] *School of Energy and Power Engineering, Jiangsu University, Zhenjiang, Jiangsu, 212013 P.R. China*
[b] *Department of Physics, Abdul Wali Khan University, Mardan, 23200 Pakistan*
[c] *Department of Chemistry, College of Science, King Saud University, Riyadh, 11451 Saudi Arabia*
**e-mail: Inamullah.k1983@gmail.com*

Received September 16, 2023; revised December 26, 2023; accepted February 12, 2024

Abstract—In this work we prepared boro-telluride glass samples while varying the concentration of TeO_2 (0.00, 10.00, 20.00 mol %) by melt quenching technique and study their physical, optical and luminescence properties by various characterization methods. We found that band gap lies in the 2.88–2.18 eV range, showing decreasing trend with increasing concentration of TeO_2. The emission spectra shows four emission peaks under 378 nm excitation centered at 486, 545, 590 and 620 nm because of the transition from $^5D_4$ state to ^7F_J (where, $J = 6, 5, 4, 3$) lower levels. Whereas the intensity decreases with increasing concentration of TeO_2, indicating that the non-radiative energy transfer through cross relaxation (CR) increases with increasing concentration of TeO_2. The color coordinates for all studied glasses fall in green region and were ($x = 0.304$, $y = 0.605$). The CCT obtained value for all prepared glasses is 6000 K. Above study suggests that these glasses can be potentially used in green light LEDs and in other solid state lighting applications.

Keywords: telluride, borate, terbium, leds, energy transfer, luminescence
DOI: 10.1134/S1087659623600825

INTRODUCTION

The rare earth (RE^{3+}) ions doped glasses are attractive due to their applications in the development of optical fiber, laser, light emitting devices, optical waveguides and amplifiers. The 4*f*–4*f* transition of RE^{3+}-ions is less sensitive to its surrounding environment because of its 4*s* and 5*p* electrons shielding properties that facilitate to obtain optical amplification and laser action in IR-region [1, 2]. The Tb^{3+}-ions doped oxide based glasses are attractive candidate for green and blue emission from emitting $^5D_4$ levels under UV-excitation. The emission from Tb^{3+}-ions doped oxide based glasses usually appear green to human vision because of the transition from $^5D_4$ to $^7F_5$ state (545 nm, green). Furthermore, these glasses are also the potential candidates for active-gain medium to obtain strong pulsed laser in green region operating at 543 nm by providing four level systems for laser with low-threshold pumping power [3–5]. Moreover, luminescence properties of the Tb^{3+}-ions have gained great attention because of its IR-to-visible up-conversion, possible excited state luminescence, large quantum yield, scintillators, display, lasers and quantum cutting [6–13]. Recently, P.W Meta et al. have reported the efficient laser operating in yellow and green regions and its saturation of green emission under visible light and cathode-ray excitation in fluoride crystal doped with Tb^{3+}-ions [12]. Yamashita et al. report the cw-laser action and amplification in fluoride fibers doped with Tb^{3+}-ions [13].

A glass former such as phosphate, borate, silicate and telluride are suitable as a glass host material of gain medium owing to their mechanical and thermal properties. Boro-tellurite host glasses are interesting material to be studied for various applications in different fields. These glasses have large refractive index, low melting temperature, good thermal and chemical stability like borate and has low phonon energy ($\approx$700 cm^{-1}), high transparency and dielectric constant as telluride has [14–18]. The introduction of network modifier such as Na_2O and CaO not only introduces the structural changes by non-bridging-oxygen (NBO) formation in boro-telluride network but also soften glass network, reduce the temperature and enhance the mechanical and chemical stability [19]. The present work aims to study the effect of glass former concentration and excitation wavelength on the

Table 1. Physical and optical properties of NCBT doped with Tb^{3+}-ions

Physical property NCBT-Tb	Glass Sample $xTeO_2$ (x = 0, 10, 20 mol %)		
	0.0	10.0	20.0
Average molecular weight, M, g/mol	71.1595	80.1575	89.1555
Density, ρ, g/cm^3	2.3089	2.4939	2.6223
Thickness of the glass, d, cm	0.3550	0.3600	0.3500
Refractive index, n_d, 589.3 nm	1.5131	1.5373	1.5533
Dielectric constant, e	2.2894	2.3633	2.4127
Optical dielectric constant, $P\partial t/\partial P$	1.2894	1.3633	1.4127
Molar volume, V_M, cm^3/mol	30.8193	32.1419	33.9989
Molar refractivity, R_m, cm^3/mol	9.2642	10.0426	10.8848
Refraction losses, R, %	4.1681	4.4843	4.6959
Molecular electronic polarizability, $\alpha_m \times 10^{-26}$ m^3	3.6712	3.9796	4.3133
Indirect optical band gap energy E_g^{ind}, eV	2.8735	2.8375	2.1792
Oxygen packing density	84.40	77.65	

luminescence properties of Tb_2O_3 (1.0 mol %) doped $10Na_2O–10CaO–(79 - x)B_2O_3–xTeO_2$ by melt quenching technique. The glass was characterized by measuring Physical, Optical and Luminescence properties by various methods and techniques.

EXPERIMENTAL

Glass sample with chemical composition of $10Na_2O–10CaO–(79 - x)B_2O_3–xTeO_2–1.0Tb_2O_3$ where x = 0, 10 and 20 mol % were prepared by melt quenching technique and labeled as NCBT00, NCBT10 and NCBT20 respectively. All chemicals were weighted according to the above composition for 5 g batch for each sample and were put into alumina crucible and melted in electric furnace at 1000°C for 3 h. The melt was then quenched at pre heated stainless steel mold and immediately transferred to another furnace for annealing at 500°C to remove the thermal stresses. Finally after cutting and polishing, the samples were characterized by various techniques.

Density of the NCBT glass samples were measured by using densitometer (Dietheim Limited, HR-200 model) using Archimedes principle with water as immersion liquid ($\rho_o = 0 : 999$ g/cm^3), refractive index was measured by Abbe refractometer (ATAGO) with mono-bromo-naphthalene as contact liquid and sodium vapor lamp providing light (λ = 598.3 nm). For structural analysis FTIR spectrometer is used. Shimadzu UV-3100 spectrometer was used to measure the absorption spectra in UV-Visible-NIR region (200 to 2500 nm). Cary Eclipse (Agilent Technologies) fluorescence spectrometer is used to measure the Lifetime, excitation and emission spectra.

RESULTS AND DISCUSSION

Physical Properties

Table 1 display optical and physical properties of the NCBT glass doped with Tb^{3+}-ions were calculated from Ref [20]. Density of material is a significant parameter used to estimate the degree of compactness of structure, modification of glass network geometrical configurations and intestinal holes dimensional variation [21]. Figure 1 shows increasing trend in density and molar volume with increasing concentration of telluride. This happens due to two reason: due to the conversion of $[BO_3]^{-3}$ triangle to BO^{-4} tetrahedral (anomaly effect of boron) and another reason is that telluride has higher molar mass and density (molar mass = 127.60 g/mol, ρ = 6.25 g/cm^3) then boron (molar mass = 10.811 g/mol, ρ = 2.34 g/cm^3). The increase in molar volume confirms the creation of non-bridging-oxygen (NBOs) and structure expansion with addition of telluride which has above density and molecular weight. The increase in density with increasing telluride concentration results in an increased in the refractive index because of the enhanced resistance to the flow of light. Oxygen packing density (OPD) is another parameter that explains the structure of network glass. The OPD decreases with the addition of telluride to the glass network indicating the expansion of the glass network expansion caused by OPD creation [23].

Fourier-Transform Infrared Spectroscopy (FTIR)

Information about the arrangement of the structural units was attained by FTIR spectroscopy. The Fig. 2 shows the FTIR spectra of NCBT glasses. There are six bands located at 805, 984, 1204, 1333, 1815–

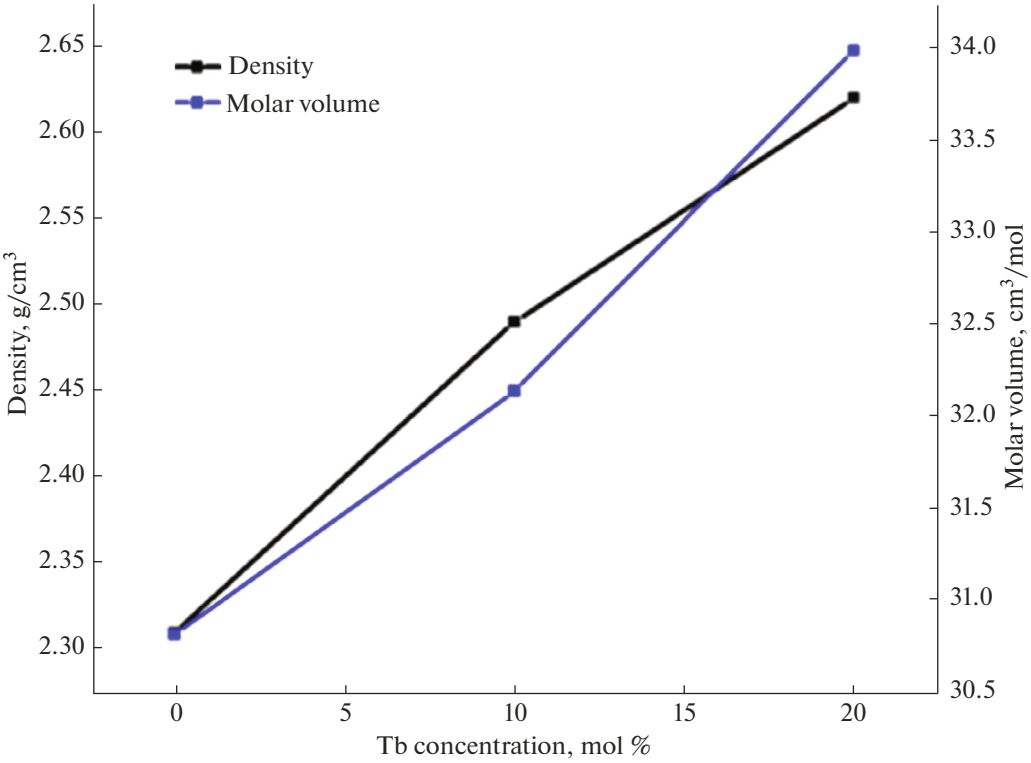

Fig. 1. Variation in molar volume and density with concentration increase of the tellurim in NCBT glasses.

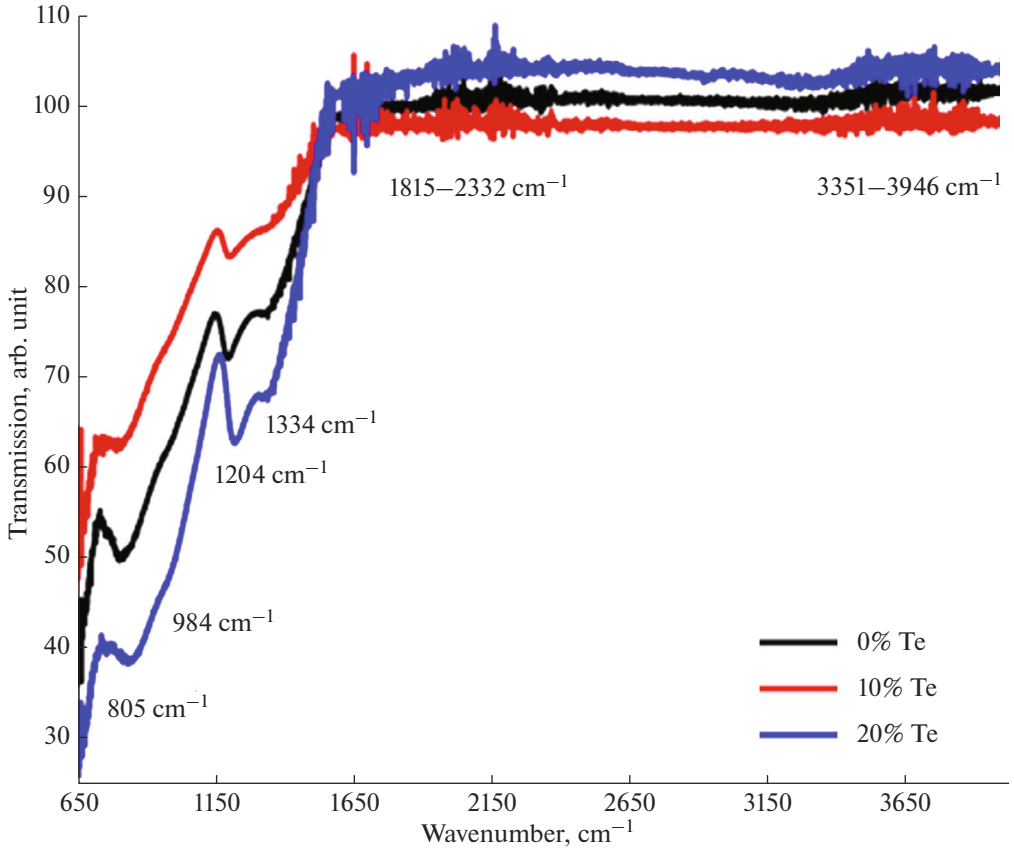

Fig. 2. FTIR spectra of Tb^{3+}-ions doped NBCT glasses.

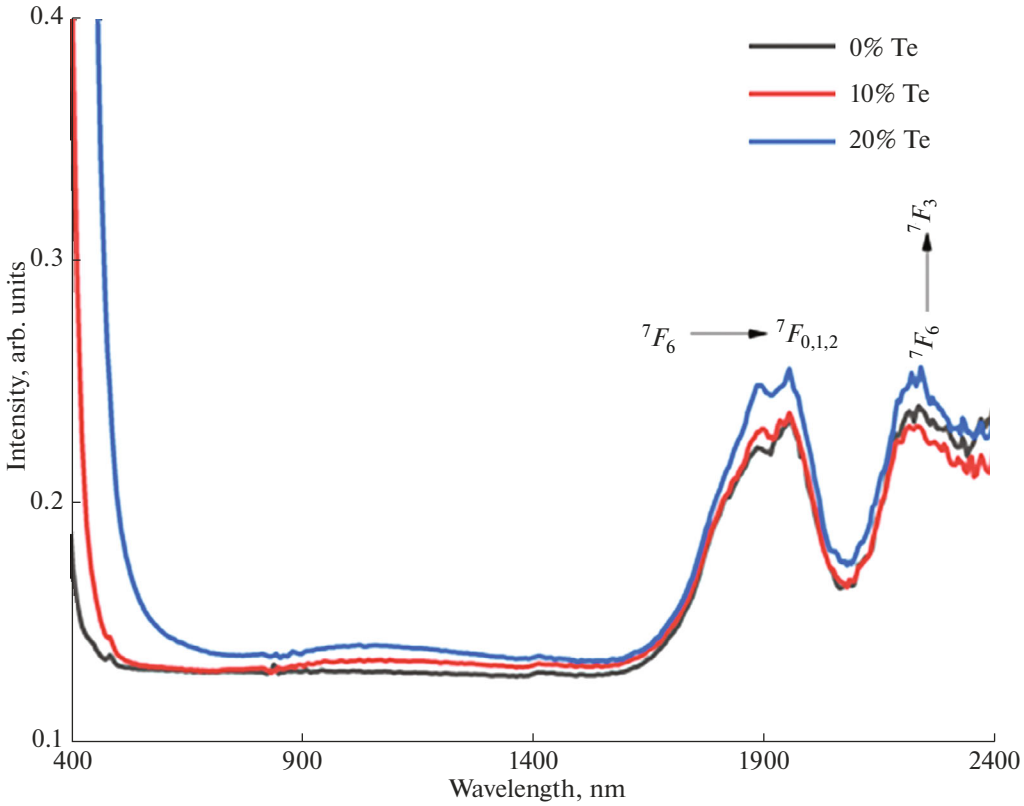

Fig. 3. Absorption spectra for Tb^{3+}-ions doped NBCT glasses.

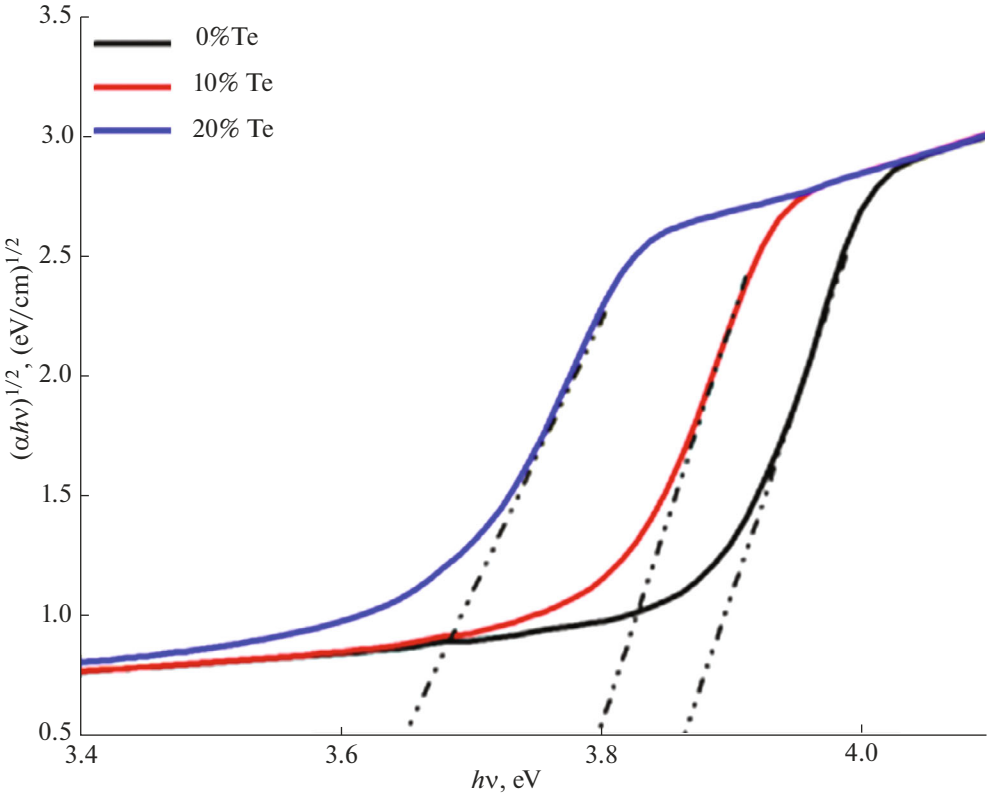

Fig. 4. Indirect band gap for Tb^{3+}-ions doped NBCT glasses.

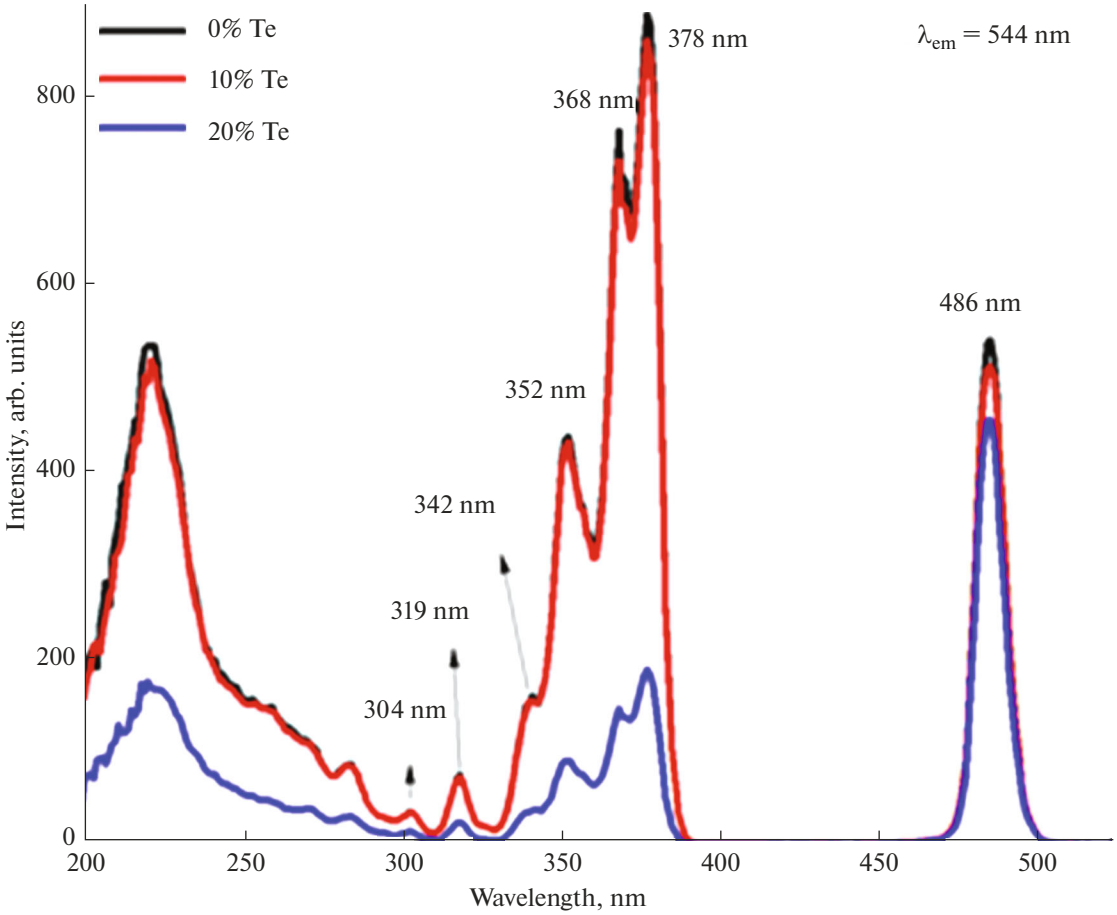

Fig. 5. Excitation spectra for Tb^{3+}-ions doped NBCT glasses.

2332 and 3351–3946 cm^{-1} in FTIR spectra of prepared NCBT glass samples. The band around 805 cm^{-1} is due to the B–O–B bond bending vibrations, while band located around 984 cm^{-1} is due to B–O bond stretching of $[BO]^4$ tetrahedral [24]. The bonds located at 1205 and 1379 cm^{-1} are due to the B–O bonds asymmetric stretching relaxation from $[BO_3]$ and pentaborate rings and tetraborate stretching vibration, respectively [24]. Moreover, the bonds at 1815–1332 and 3351–3946 cm^{-1} region are because of OH-group and H_2O anti-symmetric stretching and O–H stretching, respectively [25].

Optical Absorption and Energy Band Gap

Figure 3 shows the absorption spectra in NIR region for the prepared NCBT glasses. Where two absorption bands are observed in NIR region due to the transition to $^7F_{0,1,2}$ and $^7F_3$ levels from $^7F_6$ level. The transitions to $^7F_0$, $^7F_1$ and $^7F_2$ states from $^7F_6$ level overlap with each another. Furthermore, absorption of prepared glass increases with increase in tellurium in prepared glass samples. The peaks are assigned as per literature [3]. The indirect energy band gap (E_{opt}) was obtained by plotting $(\alpha h\nu)^n$, where ($n = 1/2$) as a function of energy of the photon ($h\nu$). Indirect band gap energy is obtained by extrapolating linear region of curve to $h\nu$-axis [3] as shown in Fig. 4. The band gap lies in the 2.88–2.18 eV range, showing decreasing trend with increasing concentration of TeO_2. The structure and chemical compositions affect the band gap of the material. The decreasing the band gap with increasing TeO_2 suggest that TeO_2 act as modifier and create NBOs in glass network. This structural disorder further results in extension of the localized states within band gap energy [26].

Excitation Spectra

Figure 5 shows the excitation spectra (for λ_{em} = 544 nm) of Tb^{3+}-ions doped NCBT glasses samples in 200–550 nm spectral range. The Fig. 5 shows broad band in 200–300 nm spectral range which originate from $4f^8$–$4f^75d$ transition of Tb^{3+}-ions [27]. Where, seven sharp peaks of Tb^{3+}-ions were observed in 300–550 nm spectral range position at 304, 319, 342, 352, 368, 378 and 486 nm due to transition from $^5F_6$ ground

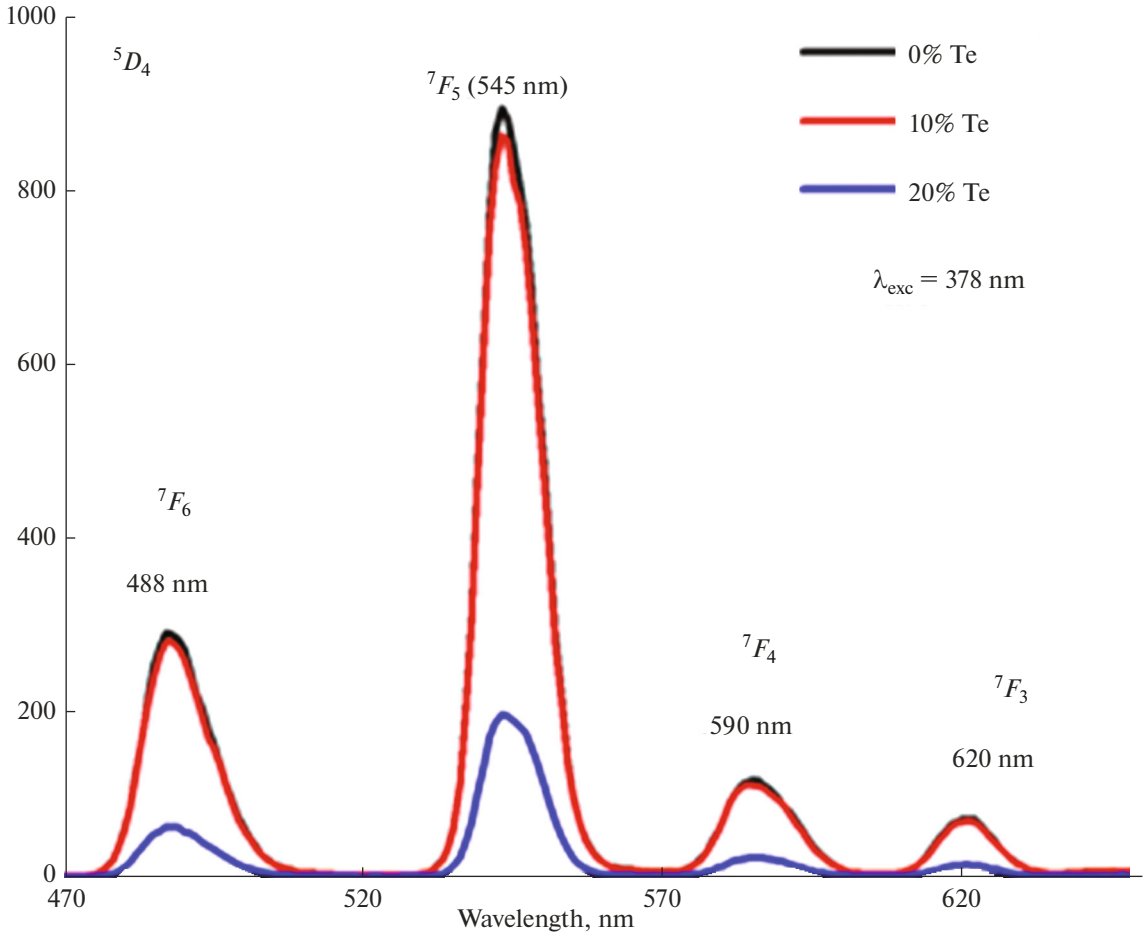

Fig. 6. Emission spectra of NCBT glasses with concentration of TeO_2 (λ_{exc} = 378 nm).

state to $^5H_6$, $^5D_1$, $^5L_{7,8}$, $^5L_6$, $^5L_{10}$, $^5D_3$ and $^5D_4$ excitation states, respectively [1]. Among these transitions, the transition to the $^5D_3$ and $^5D_4$ is more intense and hence selected to record the emission spectra of the glass samples. Whereas, another wavelength of 222 nm was selected for measuring the emission spectra of NCBT glasses doped with Tb^{3+}-ions. Similar results have also been reported in the literature [1, 3, 27].

Emission Spectra

The Figs. 6 and 7 show the emission spectra of Tb^{3+}-ions doped NCBT glasses of 10 mol % concentration of TeO_2 under 378 nm excitation and Tb^{3+}-ions doped NCBT glasses with different concentration (i.e 0.00, 10.00 and 20.00 mol %) of TeO_2 under different excitation wavelengths (i.e 222, 378 and 486 nm), respectively. The Fig. 6 shows four emission peaks under 378 nm excitation centered at 486, 545, 590 and 620 nm because of transition from $^5D_4$ state to the ^7F_J (where J = 6, 5, 4, 3) lower levels [1, 3, 12–14]. The emission positioned at 545 nm has highest intensity. Energy level diagram transition from $^5D_4$ state to the ^7F_J (where J = 6, 5, 4, 3) lower levels are shown in Fig. 8. Furthermore intensity of NCBT glass with 0.00 mol % of TeO_2 has highest intensity. Whereas the intensity decreases with increasing concentration of TeO_2, indicating that the non-radiative energy transfer through cross relaxation (CR) increases with TeO_2 addition, as shown in Fig. 8 [1, 3]. Energy transfer through CR-channel increase with increasing concentration of TeO_2 as the average-distance among Tb^{3+}–Tb^{3+} decrease because tellurium has larger size then borate which is replaced by it. Moreover the NCBT00, NCBT10 and NCBT20 glasses were pumped under 222, 378 and 486 nm excitation as shown in Figs. 7a–7c respectively. The shape and peaks position of emission spectra is independent of excitation wavelength and for all concentration of TeO_2. This is due to the intra-shielding effect of f–f transitions by 5s, 5p-orbital electrons making the 4f orbital electron of the rare earth insensitive to glass matrix. However, the emission intensity for 378 nm excitation is highest for all concentrations of TeO_2. This shows that, the non-radia-

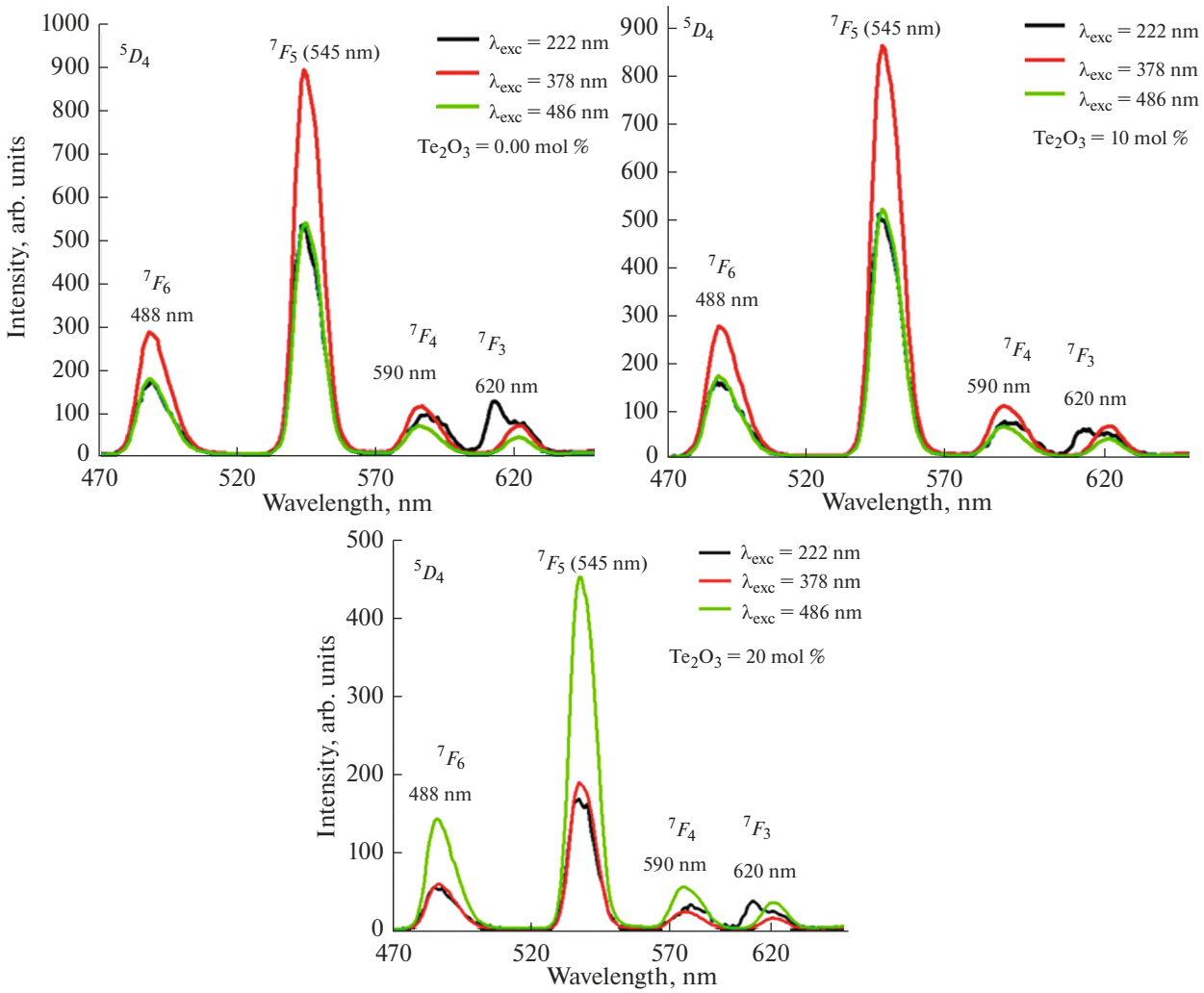

Fig. 7. Emission spectra (λ_{exc} = 222, 378 and 486 nm), of NCBT00, NCBT10 and NCBT20 glasses.

tive energy transfer (NR) and energy transfer through CR-channel are high for other excitation wavelengths.

Decay Curve Analysis

The analysis of decay curve is significant to study the interaction between donor–acceptor ions. It provides information about the luminescence quenching effect and energy transfer phenomena of the Tb^{3+}-ions [28–31]. Figure 9 shows the lifetime curve of the $^5D_4$ state of Tb^{3+}-ions in the NCBT glasses with 378 nm excitation and monitoring emission at 544 nm. It is observed that all curves for the decay time in all glasses are of single exponential. The experimental lifetime of the prepared NCBT00, NCBT10 and NCBT20 glasses are 2.73, 2.16 and 1.93 ms respectively. Furthermore, it is observed that the lifetime of $^5D_4$ state of the Tb^{3+}-ions decreases in NCBT glasses with increasing TeO_2 concentration which is due to the non-radiative energy transfer through CR-channel. Also it is expected that the multi-phonon relaxation is negligible because of wide energy gap (≈15.285 cm^{-1}) between the emitting $^5D_4$ state and next lower $^7F_0$ state.

Color Analysis

For luminescence application the color of emission from the rare earth doped glasses was study in the frame of CIE-1931 color-coordinates, a universal model of color scheme established by Commission international de l'éclairage (CIE) [32]. From the emission spectra color chromaticity coordinates were measured with 378 nm excitation for NCBT00, NCBT10 and NCBT20 samples and are shown in Fig. 10. The color coordinates for all study glasses doped with Tb^{3+}-ions fall in green region and were ($x = 0.304$, $y = 0.605$) that are very close to European-broadcasting union illuminant (EBU) green ($x = 0.290$, $y = 0.600$) [33]. Moreover the McCamy's approximation was used to estimate the quality of the emitted bright green

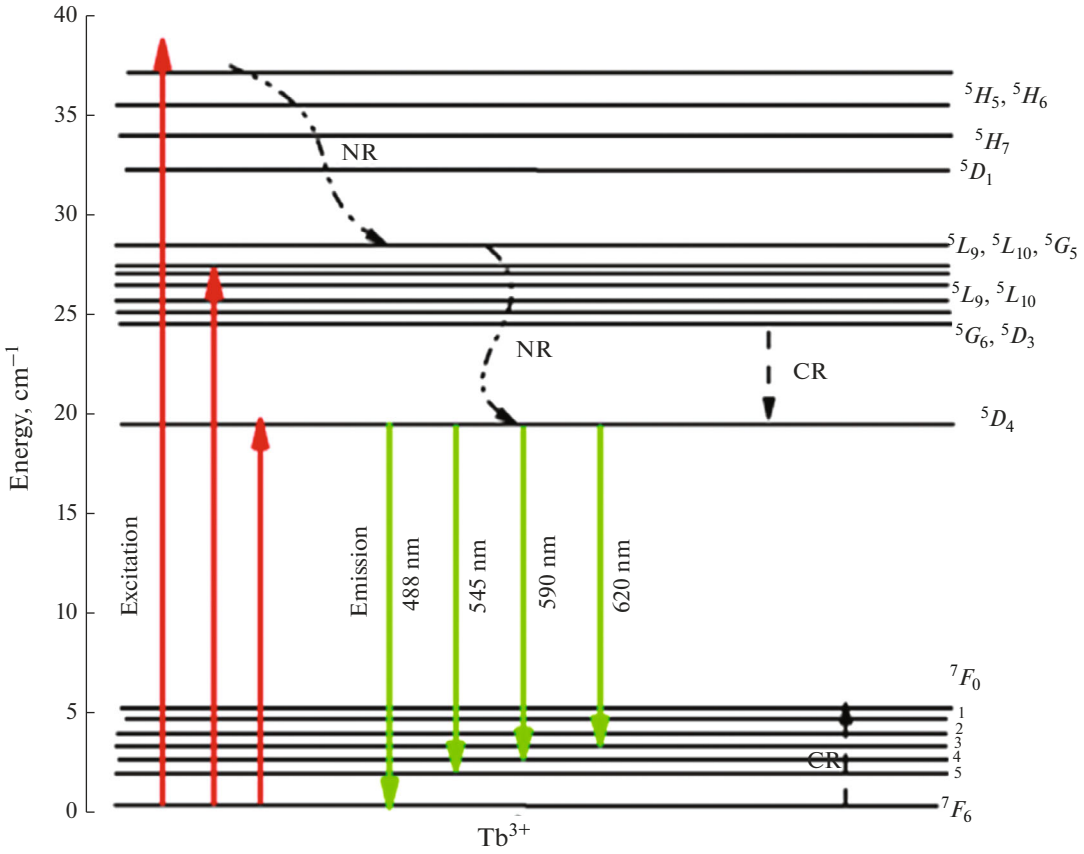

Fig. 8. Energy level diagram for Tb^{3+}-ions in the NCBT glasses.

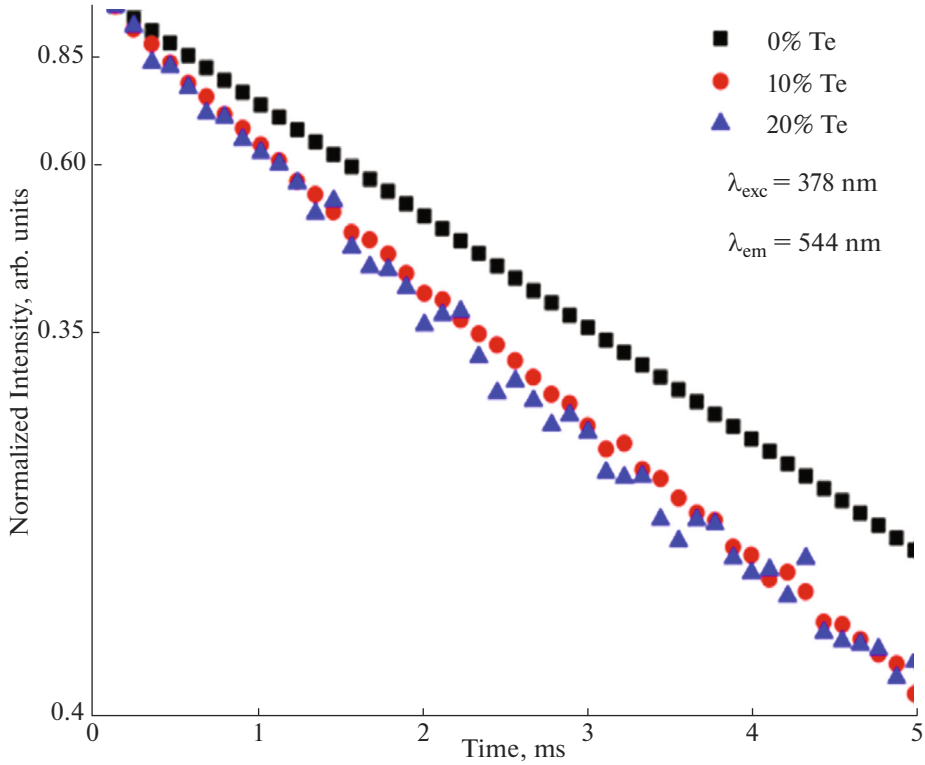

Fig. 9. Lifetime of Tb^{3+}-ions in the NCBT glasses.

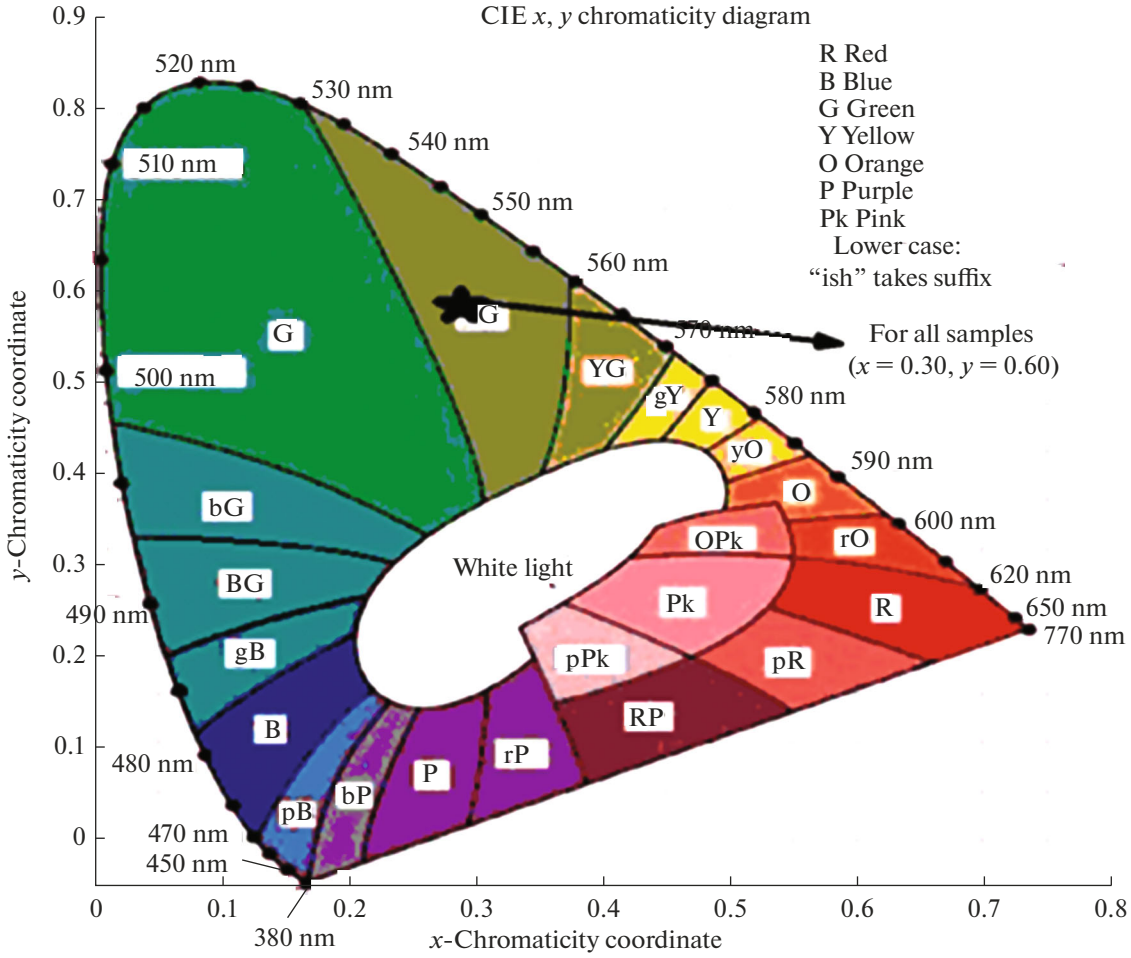

Fig. 10. CIE diagram for NCBT10 glass.

light by calculating correlated-color temperature (CCT) [34]. The CCT obtained values for all prepared glasses are 6000 K that are very close to Daylight CIE D55 (5500 K) [35] and commercial white light (6400 K) [36]. This suggests that the prepared glasses have potential application in solid state lighting technology.

CONCLUSIONS

Glass sample with chemical composition $10Na_2O$–$10CaO$–$(79 - x)B_2O_3$–$xTeO_2$–$1.0Tb_2O_3$ (where $x = 0$, 10 and 20 mol %) were prepared by melt quenching technique. While increasing molar volume with increasing TeO_2 confirms the creation of non-bridging-oxygen (NBOs) and structure expansion. This was attributed to higher density and heavier molecular weight of the telluride than those of the borate as the latter is replaced with the former. The OPD decreased with the increasing concentration of telluride to the glass network which indicates the glass network expansion. Two absorption bands were observed in the NIR region due to the transitions to $^7F_{0,1,2}$ and $^7F_3$ levels from $^7F_6$ level. The band gap lies in the 2.88–2.18 eV range, showing decreasing trend with increasing concentration of TeO_2. The excitation exhibits broad band in 200–300 nm spectral range which originating from $4f^8$–$4f^75d$ transition of the Tb^{3+}-ions. Where, seven sharp peaks of Tb^{3+}-ions were observed in 300-550 nm spectral range position at 304, 319, 342, 352, 368, 378 and 486 nm due to transition from $^5F_6$ ground state to $^5H_6$, $^5D_1$, $^5L_{7,8}$, $^5L_6$, $^5L_{10}$, $^5D_3$ and $^5D_4$ excitation states. The emission spectra showed four emission peaks under 378 nm excitation centered at 486, 545, 590 and 620 nm because of transition from $^5D_4$ state to the ^7F_J ($J = 6, 5, 4, 3$) lower levels, respectively. The intensity decreased with increasing concentration of TeO_2, showing that the non-radiative energy transfer through cross relaxation (CR) increases with increasing TeO_2 concentration. The color coordinates for all samples fall in the green region and were ($x = 0.304$, $y = 0.605$). The CCT obtained values for all samples are 6000 K. This study suggests that the prepared glasses can be potentially

used in the green-light LEDs and in other solid-state lighting applications.

FUNDING

This work was funded by the Researchers supporting project number (RSPD2024R766) King Saud University, Riyadh, Saudi Arabia. This work is also supported by the National Natural Science Foundation of China (Project number 51976081).

CONFLICT OF INTEREST

The authors of this work declare that they have no conflicts of interest.

REFERENCES

1. Kesavulu, C.R., Silva, A.C.A., Dousti, M.R., Dantas, N.O., de Camargo, A.S.S., and Catunda, T., Concentration effect on the spectroscopic behavior of Tb^{3+} ions in zinc phosphate glasses, *J. Lumin.*, 2015, vol. 165, pp. 77–84. https://doi.org/10.1016/j.jlumin.2015.04.012
2. Khan, I., Rooh, G., Ramakrishna, R., Srisittipokakun, N., Kim, H. J., and Kaewkhao, J., Energy transfer and spectroscopic investigation of Dy_2O_3 doped Li_2O–BaO–GdF_3–SiO_2 for white light LED, *Glass Phys. Chem.*, 2019, vol. 45, pp. 332–343. https://doi.org/10.1134/S1087659619050067
3. Kesavulu, C.R., Kim, H.J., Lee, S.W., Kaewkhao, J., Kaewnuam, E., and Wantana, N., Luminescence properties and energy transfer from Gd^{3+} to Tb^{3+} ions in gadolinium calcium silicoborate glasses for green laser application, *J. Alloys Compd.*, 2017, vol. 704, pp. 557–564. https://doi.org/10.1016/j.jallcom.2017.02.056
4. Kassab, L.R.P., de Almeida, R., da Silva, D.M., and de Araújo, C.B., Luminescence of Tb^{3+} doped TeO_2–ZnO–Na_2O–PbO glasses containing silver nanoparticles, *J. Appl. Phys.*, 2008, vol. 104, no. 9, p. 093531. https://doi.org/10.1063/1.3010867
5. Abdul Azeem, P., Kalidasan, M., Reddy, R.R., and Ramagopal, K., Spectroscopic investigations on Tb^{3+} doped lead fluoroborate glasses, *Opt. Commun.*, 2012, vol. 285, no. 18, pp. 3787–3791. https://doi.org/10.1016/j.optcom.2012.05.034
6. Sontakke, A.D., Biswasm K., and Annapurna, K., Concentration-dependent luminescence of Tb^{3+} ions in high calcium aluminosilicate glasses, *J. Lumin.*, 2009, vol. 129, no. 11, pp. 1347–1355. https://doi.org/10.1016/j.jlumin.2009.06.027
7. Queiroz, T.B. de, Botelho, M.B.S., Gonçalves, T.S., Dousti, M.R., and de Camargo, A.S.S., New fluorophosphate glasses co-doped with Eu^{3+} and Tb^{3+} as candidates for generating tunable visible light, *J. Alloys Compd.*, 2015, vol. 647, pp. 315–321. https://doi.org/10.1016/j.jallcom.2015.06.066
8. Vieira, T.A., dos Santos, J.F.M., Auad, Y.M., Nunes, L.A.O., Astrath, N.G.C., Baesso, M.L., and Catunda, T., Pump-induced refractive index changes in Tb^{3+} doped glasses, *J. Lumin.*, 2016, vol. 169, part B, pp. 659–664. https://doi.org/0.1016/j.jlumin.2015.07.035
9. Yamashita, T. and Ohishi, Y., Concentration and temperature effects on the spectroscopic properties of Tb^{3+} doped borosilicate glasses, *J. Appl. Phys.*, 2007, vol. 102, no. 12, p. 123107. https://doi.org/10.1063/1.2821789
10. Terra, I.A.A., Borrero-González, L.J., Nunes, L.A.O., Belançon, M.P., Rohling, J.H., Baesso, M.L., and Malta, O.L., Analysis of energy transfer processes in Yb^{3+}-Tb^{3+} co-doped, low-silica calcium aluminosilicate glasses, *J. Appl. Phys.*, 2011, vol. 110, no. 8, p. 83108. https://doi.org/10.1063/1.3653272
11. Lin, C.C., Chen, W.-T., Chu, C.-I., Huang, K.-W., Yeh, C.W., Cheng, B.-M., and Liu, R.-S., UV/VUV switch-driven color-reversal effect for Tb-activated phosphors, *Light: Sci. Appl.*, 2016, vol. 5, no. 4, p. e16066. https://doi.org/10.1038/lsa.2016.66
12. Metz, P.W., Marzahl, D.-T., Majid, A., Kränkel, C., and Huber, G., Efficient continuous wave laser operation of Tb^{3+}-doped fluoride crystals in the green and yellow spectral regions, *Laser Photonics Rev.*, 2016, vol. 10, no. 2, pp. 335–344. https://doi.org/10.1002/lpor.201500274
13. Yamashita, T. and Ohishi, Y., Amplification and lasing characteristics of Tb^{3+}-doped fluoride fiber in the 0.54 μm band, *Jpn. J. Appl. Phys.*, 2007, vol. 46, no. 11L, p. L991. https://doi.org/10.1143/JJAP.46.L991
14. Ebendor-Heidepriem, H, and Ehrt, D., Tb^{3+} *f–d* absorption as indicator of the effect of covalency on the Judd–Ofelt Ω_2 parameter in glasses, *J. Non-Cryst. Solids*, 1999, vol. 248, nos. 2–3, pp. 247–252. https://doi.org/10.1016/S0022-3093(99)00243-4
15. Eraiah, B., Optical properties of lead–tellurite doped with samarium trioxide, *Bull. Mater. Sci.*, 2010, vol. 33, pp. 391–394. https://doi.org/10.1007/s12034-010-0059-z
16. Mawlud, S.Q., Ameen, M.M., Sahar, M.R., Mahraz, Z.A.S., and Ahmed, K.F., Spectroscopic properties of Sm^{3+} doped sodium–tellurite glasses: Judd–Ofelt analysis, *Opt. Mater.*, 2017, vol. 69, pp. 318–327. https://doi.org/10.1016/j.optmat.2017.04.022
17. Selvi, S., Marimuthu, K., and Muralidharan, G., Structural and luminescence studies of Eu^{3+}:TeO_2–B_2O_3–AO–AF_2 (A = Pb, Ba, Zn, Cd, Sr) glasses, *J. Mol. Struct.*, 2017, vol. 1144, pp. 290–299. https://doi.org/10.1016/j.molstruc.2017.05.031
18. Zekri, M., Erlebach, A., Herrmann, A., Damak, K., Rüssel, C., Sierka, M., and Maâlej, R., Structure prediction of rare earth doped BaO and MgO containing aluminosilicate glasses–the model case of Gd_2O_3, *Materials*, 2018, vol. 11, p. 1790. https://doi.org/10.3390/ma11101790
19. Cormiera, L. and Neuville, D.R., Ca and Na environments in Na_2O–CaO–Al_2O_3–SiO_2 glasses: Influence of cation mixing and cation–network interactions, *Chem. Geol.*, 2004. vol. 213, nos. 1–3, pp. 103–113. https://doi.org/10.1016/j.chemgeo.2004.08.049

20. Rao, A.S., Ahammed, Y.N., Reddy, R.R., and Rao, T.V.R., Spectroscopic studies of Nd^{3+}-doped alkali fluoroborophosphate glasses, *Opt. Mater.*, 1998, vol.10, no. 4, pp. 245–252. https://doi.org/10.1016/S0925-3467(97)00055-4
21. Kashif, I., El-Maboud A.A., and Ratep, A., Effect of Nd_2O_3 addition on structure and characterization of lead bismuth borate glass, *Results Phys.*, 2014, vol. 4, pp. 1–5. https://doi.org/10.1016/j.rinp.2013.11.002
22. Pawar, P.P., Munishwar, S.R., and Gedam, R.S., Physical and optical properties of Dy^{3+}/Pr^{3+} co-doped lithium borate glasses for W-LED, *J. Alloys Compd.*, 2016, vol. 660, pp. 347–355. https://doi.org/10.1016/j.jallcom.2015.11.087
23. Khan, I., Rooh, G., Ramakrishna, R., Srisittipokakun, N., Kim, H.J., Kaewkhao, J., and Ruangtaweep, Y., Photoluminescence Properties of Dy^{3+} ion-doped Li_2O–PbO–Gd_2O_3–SiO_2 glasses for white light application, *Braz. J. Phys.*, 2019, vol. 49, no. 5, pp. 605–614. https://doi.org/10.1007/s13538-019-00695-0
24. Rada, S., Dan, V., Rada, M., and Culea, E., Gadolinium-environment in borate–tellurate glass ceramics studied by FTIR and EPR spectroscopy, *J. Non-Cryst. Solids*, 2010, vol.356. nos. 9–10, pp. 474–479. https://doi.org/10.1016/j.jnoncrysol.2009.12.011
25. Khan, I., Rooh, G., Ramakrishna, R., Sirsittapokakun, N., Kim, H.J., Kaewkhao, J., and Kirdsiri, K., Energy transfer phenomenon of Gd^{3+} to excited ground state of Eu^{3+} ions in Li_2O–BaO–Gd_2O_3–SiO_2–Eu_2O_3 glasses, *Spectrochim. Acta, Part A*, 2019, vol. 210, pp. 21–29. https://doi.org/10.1016/j.saa.2018.11.008
26. Mott, N.F. and Davis, E.A., *Electronic Processes in Non-Crystalline Materials*, Oxford: Oxford Univ. Press, 1971.
27. Sun, X.-Y., Yu, X.-G., Wang, W.-F., Li, Y.-N., Zhang, Z.-J., and Zhao, J.-T., Luminescent properties of Tb^{3+}-activated B_2O_3–GeO_2–Gd_2O_3 scintillating glasses, *J. Non-Cryst. Solids*, 2013, vol. 379, pp. 127–130. https://doi.org/10.1016/j.jnoncrysol.2013.08.002
28. Hou, D., Liang, H., Xie, M., Ding, X., Zhong, J., Su, Q., Tao, Y., Huang, Y., and Gao, Z., Bright green-emitting, energy transfer and quantum cutting of $Ba_3Ln(PO_4)_3$:Tb^{3+} (Ln = La, Gd) under VUV-UV excitation, *Opt. Express*, 2011, vol. 19, no. 12, pp. 11071–11083. https://doi.org/10.1364/OE.19.011071
29. Duan, Q., Qin, F., Wang, D., Xu, W., Cheng, J., Zhang, Z., and Cao, W., Quantum cutting mechanism in Tb^{3+}–Yb^{3+} co-doped oxyfluoride glass, *J. Appl. Phys.*, 2011, vol. 110, p. 113503. https://doi.org/10.1063/1.3662916
30. Vermelho, M.V.D., dos Santos, P.V., de Araújo, M.T., Gouveia- Neto, A.S., Cassanjes, F.C., Ribeiro, S.J.L., and Messaddeq, Y., Thermally enhanced cooperative energy-transfer frequency upconversion in terbium and ytterbium doped tellurite glass, *J. Lumin.*, 2003, vols. 102–103, pp. 762–767. https://doi.org/10.1016/S0022-2313(02)00638-5
31. Pisarski, W.A., Żur, L., Sołtys, M., and Pisarska, J., Terbium-terbium interactions in lead phosphate glasses, *J. Appl. Phys.*, 2013, vol.113, p. 143504. https://doi.org/10.1063/1.4799592
32. Schubert, E.F., *Light Emitting Diodes*, Cambridge: Cambridge Univ. Press, 2006, Chapter 17, p. 292.
33. Juárez-Batalla, J., Meza-Rocha, A.N., Muñoz, H.G., Camarillo, I., and Caldiño, U., Luminescence properties of Tb^{3+}-doped zinc phosphate glasses for green laser application, *Opt. Mater.*, 2016, vol. 58, pp. 406–411. https://doi.org/10.1016/j.optmat.2016.06.022
34. McCamy, C.S., Correlated color temperature as an explicit function of chromaticity coordinates, *Color. Res. Appl.*, 1992, vol. 17, no. 2, pp. 142–144. https://doi.org/10.1002/col.5080170211
35. Fuchs, E.C., Sommer, C., Wenzl, F.P., Bitschnau, B., Paulitsch, A.H., Mühlanger, A., and Gatterer, K., Poly spectral white light emission from Eu^{3+}, Tb^{3+}, Dy^{3+}, Tm^{3+} co-doped $GdAl_3(BO_3)_4$ phosphors obtained by combustion synthesis, *Mater. Sci. Eng., B*, 2009, vol. 156, nos. 1–3, pp. 73–78. https://doi.org/10.1016/j.mseb.2008.11.024
36. Yang, C.H., Pan, Y.X., and Zhang, Q.Y., Enhanced white light emission from Dy^{3+}/Ce^{3+} codoped $GdAl_3(BO_3)_4$ phosphors by combustion synthesis, *Mater. Sci. Eng., B*, 2007, vol. 13, pp. 195–199.